NASA

Technical Memorandum 86125

SAN MARCO D/L SOLAR ARRAY SYSTEM DESIGN AND PERFORMANCE

Maurizio Di Ruscio, Alessandro Agneni, and John H. Day, Jr.

JUNE 1984

National Aeronautics and Space Administration

Goddard Space Flight Center
Greenbelt, Maryland 20771

TM 86125

SAN MARCO D/L SOLAR ARRAY SYSTEM DESIGN AND PERFORMANCE

John H. Day, Jr.
NASA Goddard Space Flight Center
Greenbelt, Maryland

Maurizio Di Ruscio and Alessandro Agneni
CRA, University of Rome
Rome, Italy

June 1984

GODDARD SPACE FLIGHT CENTER
Greenbelt, Maryland

CONTENTS

INTRODUCTION

The San Marco D/L spacecraft (scheduled for launch in 1985) is a scientific satellite designed to study the layer structure of the upper atmosphere[1]. The spacecraft configuration is illustrated in Figure 1 and its main characteristics are given below.

Size: approximates a sphere of 1 meter in diameter

Weight: 240 Kg

Orbit: equatorial, 290 Km × 800 Km

Spin: 6 rpm about the Z axis

Lifetime: 18 months

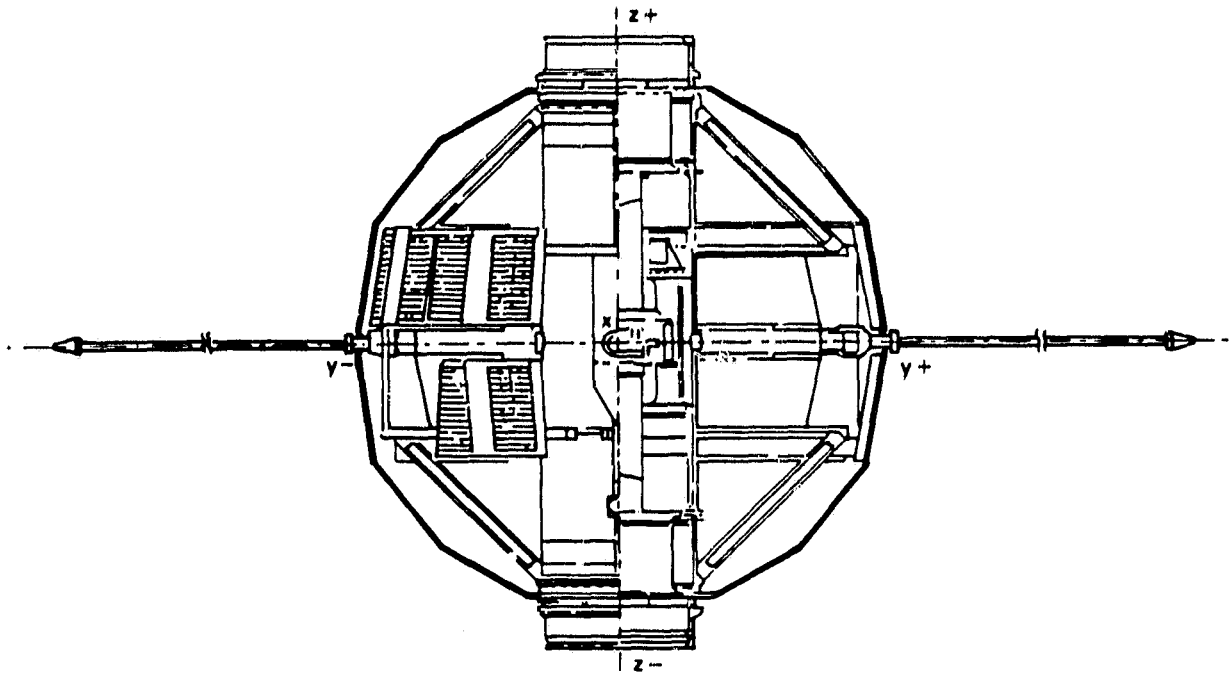

FIGURE 1. SAN MARCO D/L SPACECRAFT CONFIGURATION

The San Marco D/L power system[2] consists of a solar array, rechargeable nickel cadmium batteries, the spacecraft loads, and associated control and regulation circuitry. The spacecraft load requirements are approximately 2.7 watts continuous and 70 watts on command. However, typical data acquisition and data dumping load conditions range from 35 watts to 65 watts. It was not a design requirement for the solar array to support 100% science for an entire orbit at beginning of life (BOL) or end of life (EOL). Because San Marco D/L is very small and because of unique design constraints, the spacecraft cannot support a comparatively large solar array. Hence, the San Marco D/L solar array was designed with the requirement that duty cycling of on-command loads be performed to balance the power budget.

ARRAY DESIGN LIMITATIONS

In addition to the spacecraft power requirements, a major design consideration for the San Marco D/L solar array system was compatibility with the "Drag Balance" experiment[3]. This experiment consists of a very elastic system which transmits and measures the aerodynamic forces exerted on the outer shell. The local air density is then determined from the drag force measurement. Three requirements must be met in order to achieve a very high sensitivity in the drag balance measurement system:

a) the outer shell of the spacecraft must be light weight and rigid;

b) the external shape of the spacecraft must approach the shape of a sphere without large area appendages (however, it was necessary to mount 4 booms on the spacecraft equatorial plane to obtain the proper moment of inertia ratios amoung the 3 principal axes);

c) the outer shell of the the spacecraft must be a free body except for the drag balance which elastically connects it to the main body.

For the above reasons, it was not possible to use solar paddles or to mount solar panels directly on the outer shell of the spacecraft. The solution[4], as employed on San Marco C spacecraft, was to mount the solar array panels on the main body behind windows to allow illumination by the sun.

MECHANICAL LAYOUT

As shown in Figure 2, the San Marco D/L solar array system consists of 28 solar cell panels distributed in 2 loops, 1 above and 1 below the equator of the spacecraft. The panels are mounted on supports all of which are planar except for 2 which are conical. Solar cell panels in the upper and lower loops are inclined $+9°$ and $-9°$, respectively, corresponding to the inclinations of the upper and lower truncated cones which form the equatorial portion of the outer shell.

Layout of the solar array panels/windows is compatible with the position of the experiments and the spacecraft geometry. Most of the experiment sensors are located along an area of the spacecraft, causing a nonuniform distribution and a limitation in window dimensions and layout.

FLIGHT EXPERIMENT

The San Marco D/L solar array consists of 2 identical sections of 14 parallel connected panels, 13 Si solar cell panels and 1 GaAs solar cell panel. As shown in Figure 3, each section consists of consecutive connected panels alternating from the upper and lower loops so that the spin-averaged output current for the 2 sections will be equal for all sun angles. The only allowed exception is for the solar array flight experiment in which the in-flight performance of Si and GaAs solar cell panels will be compared. The panels are required to be physically located together and electrically connected to the same operating point. The performances of only 1 pair (1 Si and 1 GaAs) of panels will be monitored in flight. Power system measurements that will be made available by spacecraft telemetry are illustrated in Figure 4. The parameters associated with the solar array flight experiment are:

a) T_{GaAs}, GaAs panel temperature

b) T_{Si}, Si panel temperature

c) I_{GaAs}, GaAs panel current

d) I_{Si}, Si panel current

e) V_{SCT}, section voltage (GaAs & Si panel operating point)

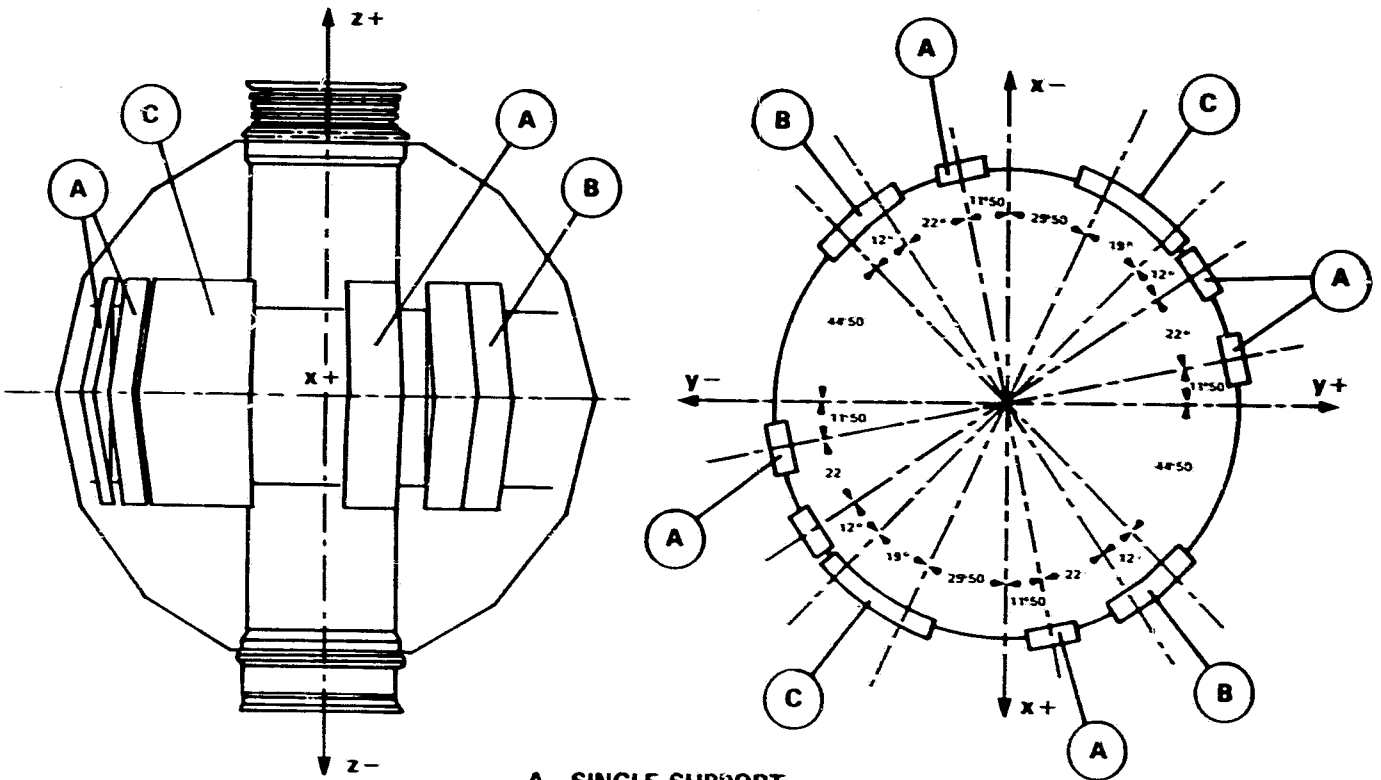

FIGURE 2. DISTRIBUTION OF THE SAN MARCO D/L SOLAR PANELS

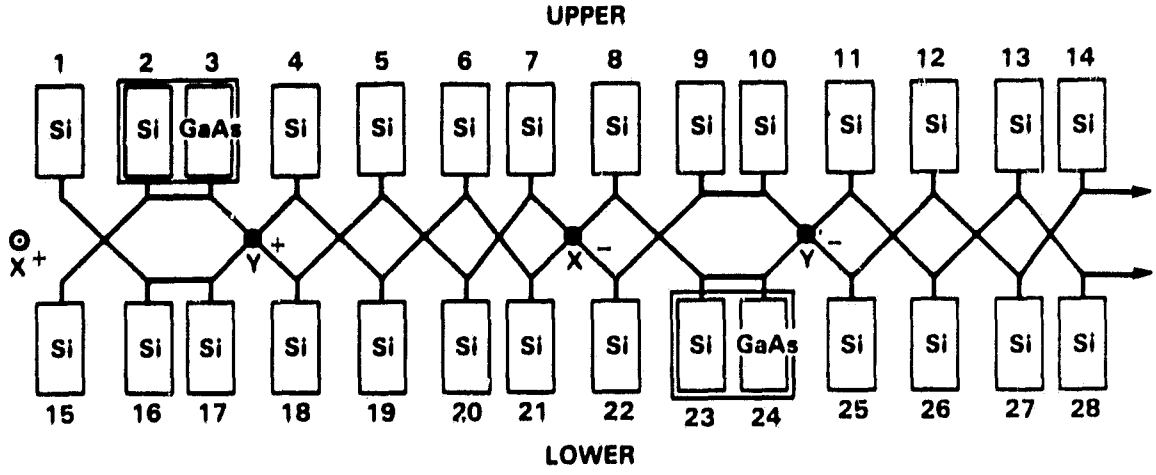

FIGURE 3. SOLAR PANELS ELECTRICAL CONNECTION

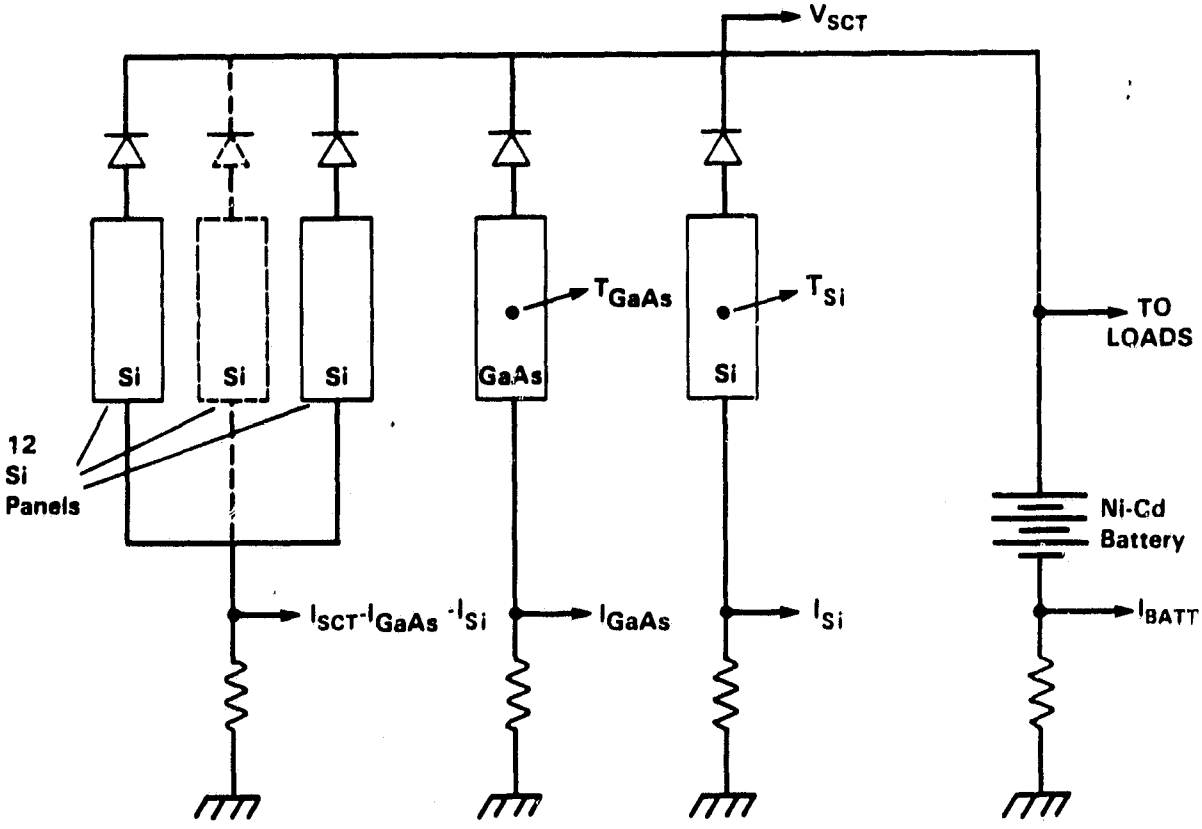

FIGURE 4. POWER SYSTEM ELECTRICAL MEASUREMENTS

PANEL DESCRIPTION

The GaAs panels were supplied for San Marco D/L courtesy of the U.S. Air Force Aero Propulsion Laboratory (USAFAPL). A total of 5 GaAs solar cell panels were manufactured for San Marco D/L. The manufacturer performed qualification tests on 1 panel. The remaining 4 panels were evaluated for flight[5] by NASA Goddard Space Flight Center (GSFC). Two of the four panels were recommended for flight.

As shown in Figure 5, each GaAs solar cell panel consists of 28 2cm × 2 cm cells connected in series. The GaAs solar cells were fabricated by the USAFAPL contractor[6] using their liquid phase epitaxial growth technique which has consistently produced 16 percent to 18 percent air mass zero (AMO) efficient GaAs solar cells. In addition to the conventional cell layers (substrate, n-doped, and p-doped), this GaAs solar cell structure includes an (AlGa)As window layer that reduces carrier recommendation near the GaAs surface to achieve high efficiency. The characteristics of the typical San Marco D/L GaAs solar cell are given in Table 1.

Each Si solar cell panel consists of a series string of 56 2cm × 1cm cells (Figure 6). The cell type is a conventional Spectrolab K7 Si cell[7]. Its characteristics are given in Table 2. As with the GaAs cells, the Si cells are connected in series with conventional stress-relief interconnects and adhered to a 170mm × 84.3mm micaply insulated aluminum panel. Each panel has 4 mounting holes and 2 electrical feed-thru terminals (1 positive and 1 negative). The terminals are accessible from the rear of the panel where they are connected to a printed circuit board on which the blocking diode is mounted.

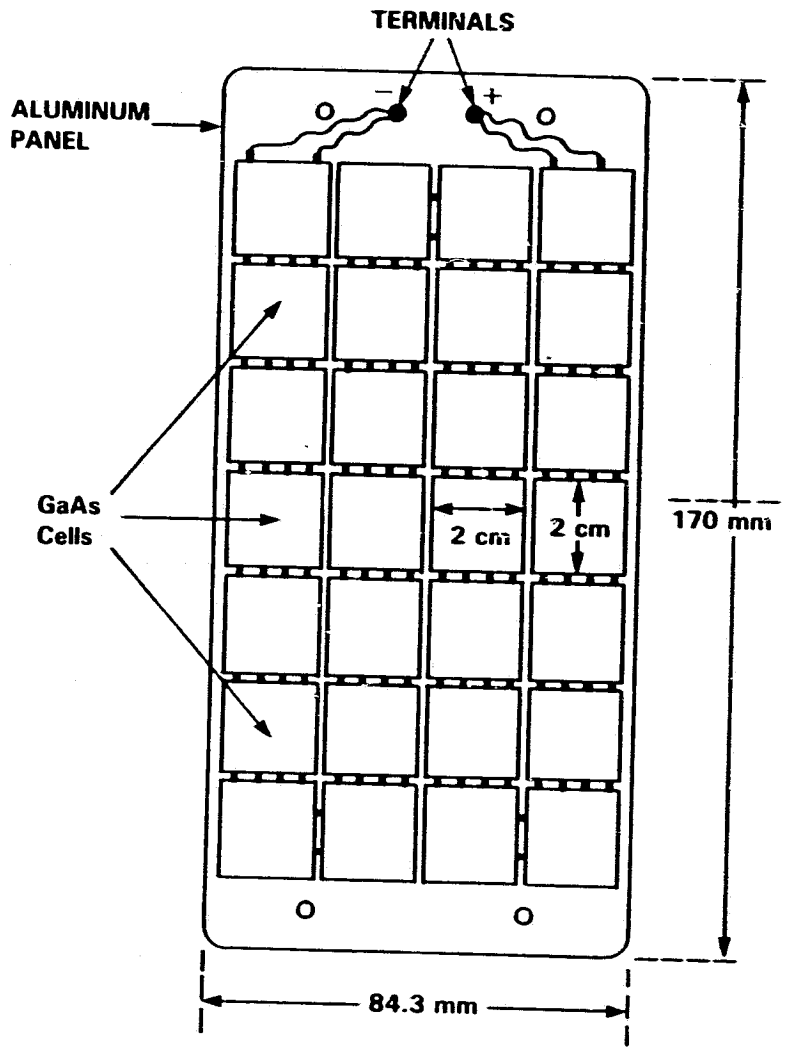

FIGURE 5. GaAs SOLAR CELL PANEL

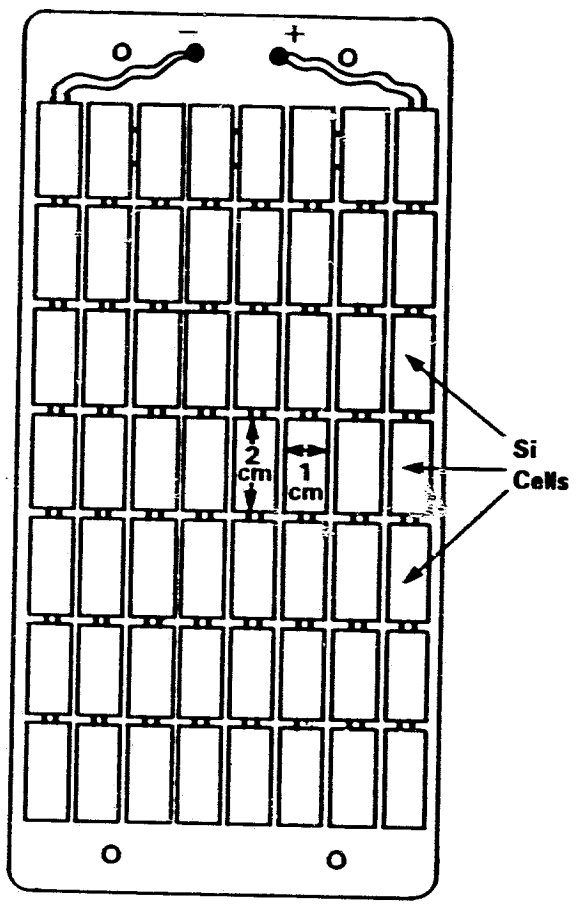

FIGURE 6. Si SOLAR CELL PANEL

Table 1
GaAs Cell Characteristics

Property	Description
n contact	(Au-Ge-Ni) Ag
Substrate layer	GaAs, Te-doped
n layer	GaAs, Sn-doped
P layer	GaAs, Be-doped
Window layer	(AlGa) As, Be-doped
P contact	(Au-Zn) Ag
AR coating	Ta_2O_5
Cell area	2cm × 2cm
Cell thickness	.03cm
Coverglass thickness	.03cm

Table 2.
Si Cell Characteristics

Property	Description
P contact	Al-Ti-Pd-Ag
Back surface layer	P+ field, red reflector
P substrate	Si, Bo-doped
n layer	Si, P-doped
n contact	Ti-Pd-Ag
AR coating	Ta_2O_5
Cell area	2cm × 1cm
Cell thickness	.03cm
Coverglass thickness	.03cm

PANEL PERFORMANCE BEFORE IRRADIATION

Each GaAs solar cell panel was exposed to AMO solar illumination, as simulated by a pulsed Xenon source. The intensity calibration was performed with a 2cm × 2cm silicon solar cell (balloon standard) that was thermally anchored at 28°C. The current-voltage (I-V) data were acquired during the light pulse while external load resistances were switched electronically. The measured I-V curve and performance parameters for the GaAs panel at 28°C are given in Figure 7.

The beginning of life (BOL) performance of the Si solar cell panel has been provided by the manufacturer[8]. The I-V curve for the typical Si panel at 28°C and AMO solar illumination is shown in Figure 8. It should be noted that for the San Marco D/L solar array the peak power output of the typical Si panel is approximately 20% less than the peak power output of the GaAs panel at BOL, 28°C, & AMO solar illumination.

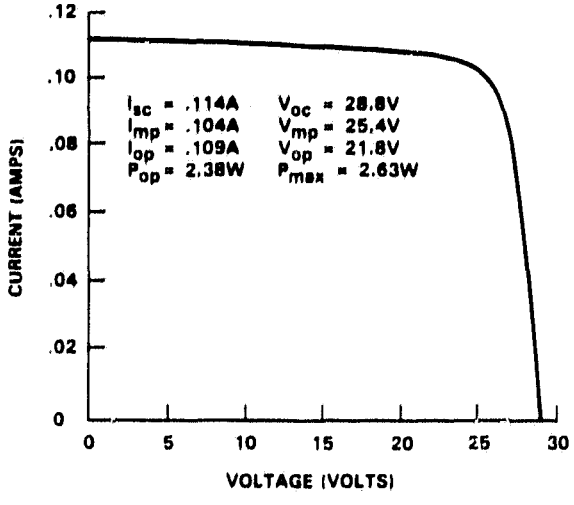

FIGURE 7. GaAs PANEL PERFORMANCE AT BOL, 28°C AND AMO SOLAR ILLUMINATION[5]

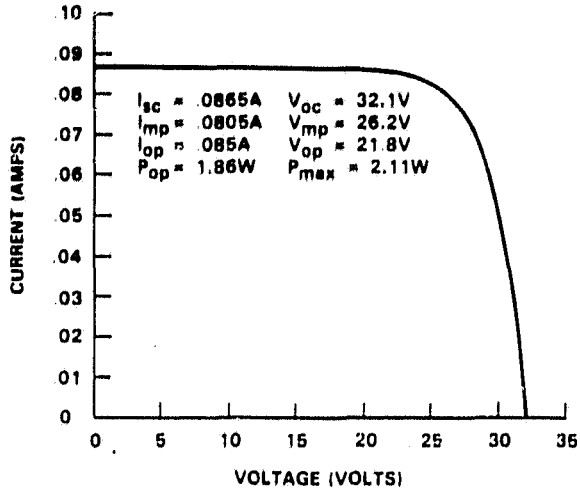

FIGURE 8. Si PANEL PERFORMANCE AT BOL, 28°C AND AMO SOLAR ILLUMINATION[8]

CHARGED-PARTICLE IRRADIATION DOSAGE

A study has been performed[9] to determine the San Marco D/L radiation environment. A worst case orbit (period, 100 minutes; inclination, 3 degrees; perigee, 290 kilometers; apogee, 1400 kilometers) was integrated over the then most current space radiation models to estimate the charge particle flux. The results for electron and proton radiations are given in Tables 3 and 4, respectively.

Much is known about the degradation of solar cells due to irradiation with monoenergetic unidirectional charged particles. However, the space radiation environment consists of a spectrum of omnidirectional charged particles. Hence, a method[10] has been used in which the above multienergetic omnidirectional space radiation fluences $\Phi(>E_1)...\Phi(>E_n)$ may be converted to an equivalent 1 Mev normal incident electron fluence $\psi(t)$ for a given shielding thickness t.

$$\psi(t)_{1\ Mev,\ e} = \sum_{E=0}^{\infty} \left[\phi(>E+dE/2) - \phi(>E-dE/2)\right] \bullet D(E,t)$$

where $D(e,t)...D(\infty, t)$ are radiation damage coefficients for shielding of thickness t. The San Marco D/L Si and GaAs solar cells are shielded by .03 cm thick fused silica coverglasses. The damage coefficients (Tables 5 and 6) corresponding to this shielding thickness were interpolated from handbook tables[10]. Upon substituting the damage coefficients and radiation environment data for 18 months into the above equation, the resulting fluences for the San Marco D/L solar array are 3.78E+13 1 Mev e^-/cm^2 and 4.59 E+13 1 Mev e^-/cm^2 for Isc and Voc, respectively. It should be noted that the validity of an equivalent electron fluence for GaAs solar cells is under scrutiny[11]. Thus, the accuracy of this estimate is subject to verification by the flight experiment.

Table 3
Electron Radiation Environment[9]

Energy (>Mev)	Worst Case Flux (electrons/cm²/day)	Energy (>Mev)	Worst Case Flux (electrons/cm²/day)
0.10	1.291E+11	0.20	7.069E+10
0.30	3.047E+10	0.40	1.032E+10
0.50	3.502E+ 9	0.60	1.918E+ 9
0.70	1.054E+ 9	0.80	6.498E+ 8
0.90	4.488E+ 8	1.00	3.102E+ 8
1.25	1.708E+ 8	1.50	9.417E+ 7
1.75	6.228E+ 7	2.00	4.119E+ 7
2.25	2.693E+ 7	2.50	1.765E+ 7
2.75	9.158E+ 6	3.00	4.776E+ 6
3.25	1.580E+ 6	3.50	5.318E+ 5
3.75	1 824E+ 5	4.00	5.273E+ 4
4.25	1.382E+ 4		

Table 4.
Proton Radiation Environment[9]

Energy (>Mev)	Worst Case Flux (electrons/cm²/day)	Energy (>Mev)	Worst Case Flux (electrons/cm²/day)
2	1.058E+8	3	1.042E+8
4	1.027E+8	5	1.012E+8
6	9.969E+7	8	9.610E+7
10	9.266E+7	15	8.505E+7
20	7.815E+7	25	7.361E+7
30	6.934E+7	35	6.645E+7
40	6.368E+7	45	6.103E+7
50	5.850E+7	55	5.615E+7
60	5.391E+7	70	4.968E+7
80	4.580E+7	90	4.222E+7
100	3.893E+7	125	3.139E+7
150	2.532E+7	175	2.044E+7
200	1.651E+7	250	1.062E+7
300	6.833E+6	350	4.401E+6
400	2.836E+6	500	1.180E+6

Table 5
Electron Damage Coefficients[10]

Energy (Mev)	Damage Coefficent	Energy (Mev)	Damage Coefficient
0.250	0.00	0.350	2.05E−4
0.450	3.25E−3	0.550	1.81E−2
0.650	4.36E−2	0.750	8.12E−2
0.850	1.28E−1	0.950	1.82E−1
1.125	2.84E−1	1.375	4.48E−1
1.625	6.39E−1	1.875	8.48E−1
2.125	1.07E+0	2.375	1.30E+0
2.625	1.53E+0	2.875	1.77E+0
3.125	2.01E+0	3.375	2.24E+0
3.625	2.47E+0	3.875	2.70E+0
4.125	2.93E+0		

Table 6
Proton Damage Coefficients[10]

Energy (Mev)	Damage Coefficients	
	I_{SC}	V_{OC} and P_{MAX}
5.5	0.00	0.00
7.0	7.16E−2	1.95E−1
9.0	3.08E−1	8.00E−1
12.5	3.68E−1	6.11E−1
17.5	3.65E−1	4.50E−1
22.5	3.77E−1	4.17E−1
27.5	3.79E−1	4.00E−1
32.5	3.72E−1	3.85E−1
37.5	3.60E−1	3.69E−1
42.5	3.48E−1	3.54E−1
47.5	3.34E−1	3.38E−1
52.5	3.20E−1	3.23E−1
57.5	3.06E−1	3.09E−1
65.0	2.87E−1	2.89E−1
75.0	2.62E−1	2.63E−1
85.0	2.39E−1	2.39E−1
95.0	2.15E−1	2.16E−1
112.5	1.82E−1	1.82E−1
137.5	1.44E−1	1.44E−1
162.5	1.18E−1	1.18E−1
187.5	1.01E−1	1.01E−1
225.0	7.62E−2	7.62E−2
275.0	4.27E−2	4.27E−2
325.0	9.18E−3	9.18E−3
375.0	0.00	0.00

PANEL PERFORMANCE AFTER IRRADIATION

Degradation of the I-V parameters for the San Marco D/L solar cells as a function of normal incident 1 Mev electron fluence has been documented[12,13]. These data are given in Figures 9, 11, and 13 for the Si cells and Figures 10, 12, 14 for the GaAs cells. The percentage degradation of each I-V parameter due to previously calculated EOL irradiation dosage is determined from the above data. The resulting I-V parameters after irradiation are given in Table 7. The operating point current was determined from the equation below, which approximates the shape of an I-V curve[14].

$$I = I_{sc} \bullet (1 + c_1 \bullet (1 - \mathrm{Exp}\,[V/(c_2 \bullet V_{oc})]))$$

where $c_1 = [1 - (I_{mp}/I_{sc})] \bullet \mathrm{Exp}[-V_{mp}/(c_2 \bullet V_{oc})]$

and $c_2 = [(V_{mp}/V_{oc}) - 1]/\ln [1 - (I_{mp}/I_{sc})]$

Table 7
I-V Parameters at 28 °C and AMO Solar Illumination After Irradiation

I-V Parameter	Si Panel	GaAs Panel
I_{SC} (A)	.083	.111
V_{OC} (V)	30.3	28.1
P_{MAX} (W)	1.88	2.53
I_{MP} (A)	.077	.101
V_{MP} (V)	24.5	25.1
V_{OP} (V)	21.8	21.8
I_{OP} (A)	.082	.106
P_{OP} (W)	1.78	2.32

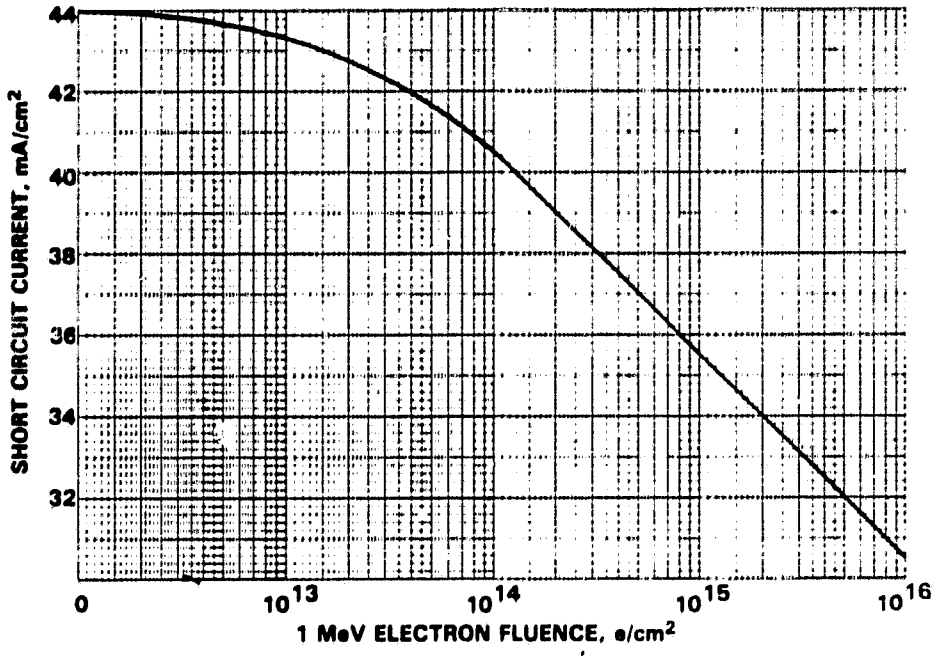

FIGURE 9. SHORT CIRCUIT CURRENT DENSITY VS 1 MeV ELECTRON FLUENCE[12]
AT 135.3 mW/cm^2 AMO ILLUMINATION, 28°C
(Si SOLAR CELL)

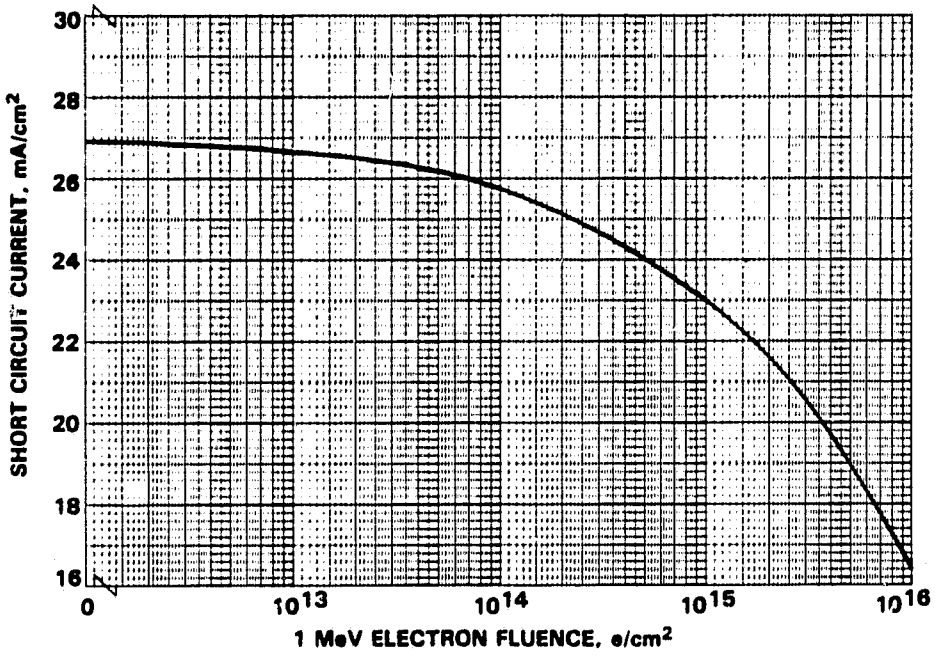

FIGURE 10. SHORT CIRCUIT CURRENT DENSITY VS 1 MeV ELECTRON FLUENCE[13]
AT 135.3 mW/cm^2 AMO ILLUMINATION, 28°C
(GaAs SOLAR CELL)

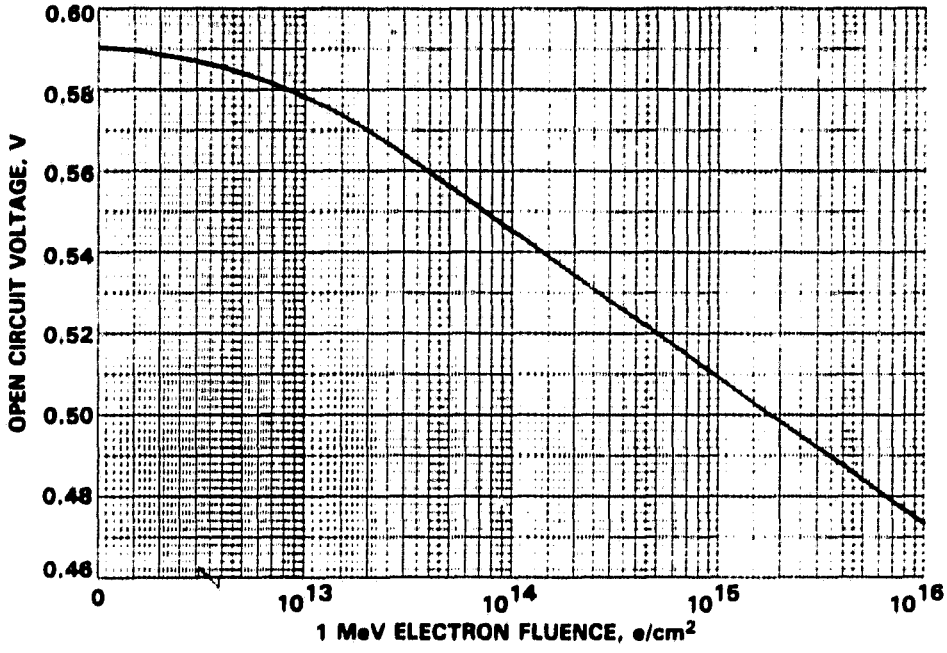

FIGURE 11. OPEN CIRCUIT VOLTAGE VS 1 MeV ELECTRON FLUENCE [12]
AT 135.3 mW/cm^2 AMO ILLUMINATION, 28°C
(Si SOLAR CELL)

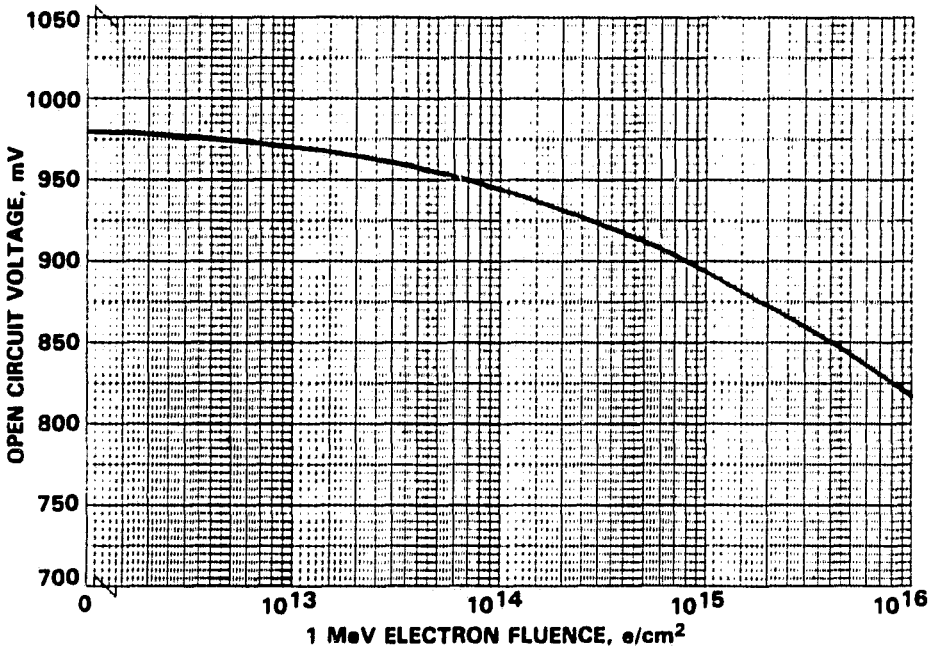

FIGURE 12. OPEN CIRCUIT VOLTAGE VS 1 MeV ELECTRON FLUENCE [13]
AT 135.3 mW/cm^2 AMO ILLUMINATION, 28°C
(GaAs SOLAR CELL)

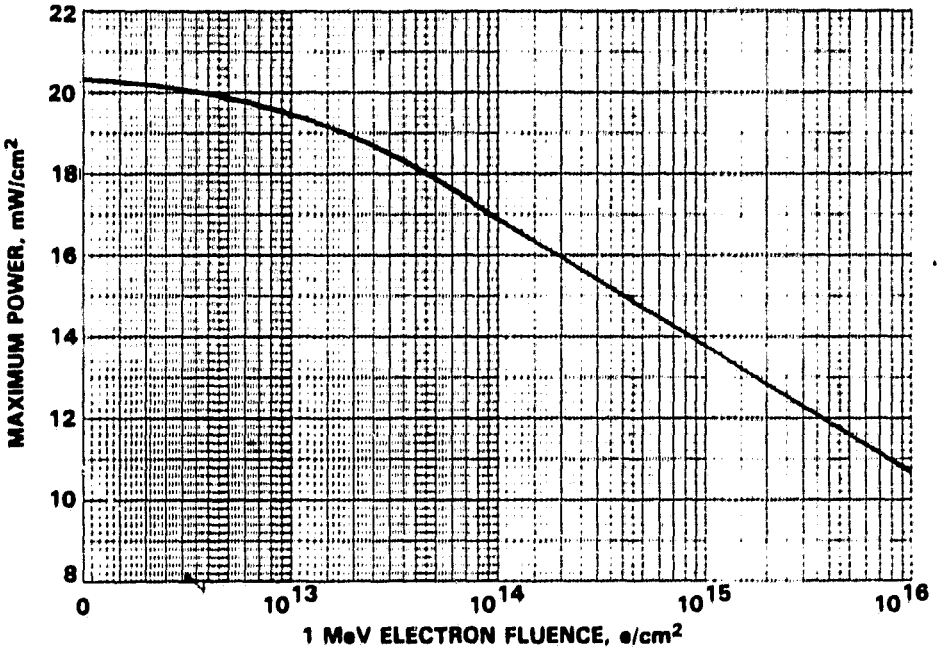

FIGURE 13. MAXIMUM POWER DENSITY VS 1 MeV ELECTRON FLUENCE [12]
AT 135.3 mW/cm² AMO ILLUMINATION, 28°C
(Si SOLAR CELL)

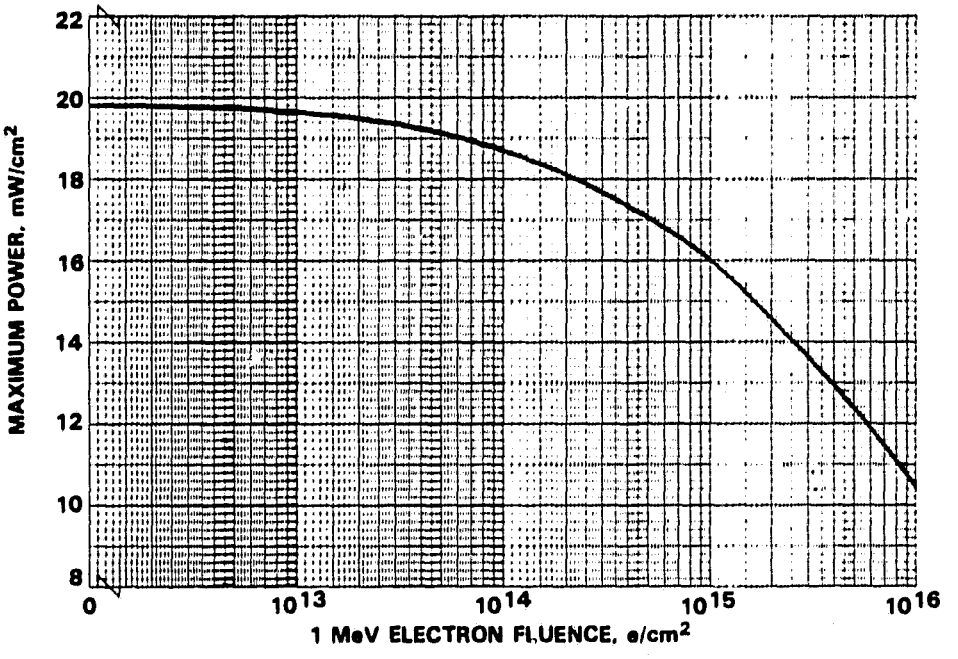

FIGURE 14. MAXIMUM POWER DENSITY VS 1 MeV ELECTRON FLUENCE [13]
AT 135.3 mW/cm² AMO ILLUMINATION, 28°C
(GaAs SOLAR CELL)

PANEL TEMPERATURE EFFECTS

The San Marco D/L solar array panels may be exposed to an operating temperature as high as 45 °C. In order that the solar array not experience a substantial loss in output, the highest possible operating voltage (21.8V) must remain below the peak power voltage when the panel reaches its highest temperature. The solar cell panel performance parameters at an arbitrary temperature are extrapolated from the performance parameters at 28 °C using temperature coefficients. The resulting AMO performance parameters as a function of temperature are given in Table 8 for the Si and GaAs panels. The output currents for the Si and GaAs panels as a function of temperature are displayed in Figures 15 and 16, respectively. The I-V data for these estimates were generated by substituting the temperature dependent I-V parameters into the curve fitting function given in the previous section.

Table 8.
Performance Parameters Versus Temperature at AMO Solar Illumination

Temperature Dependent I-V Parameters	Si Panel	GaAs Panel
I_{SC} (T) V_{OC} (T) P_{MAX} (T)	I_{SC} (28 °C) + 4.36E-5A/ °C (T-28 °C) V_{OC} (28 °C) − .1206V/ °C (T-28 °C) P_{MAX} (28 °C) − 9.97E-3W/ °C (T-28 °C)	I_{SC} (28 °C) + 6.20E-5A/ °C (T-28 °C) V_{OC} (28 °C) − .0577V/ °C (T-28 °C) P_{MAX} (28 °C) − 4.03E-3W/ °C (T-28 °C)

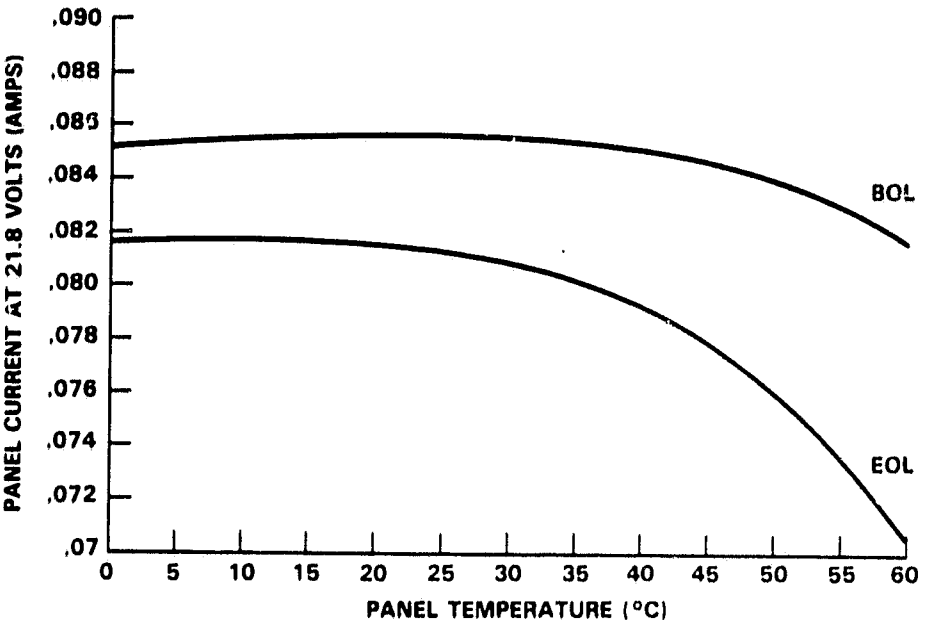

FIGURE 15. Si PANEL OUTPUT VS TEMPERATURE
AT AMO SOLAR ILLUMINATION

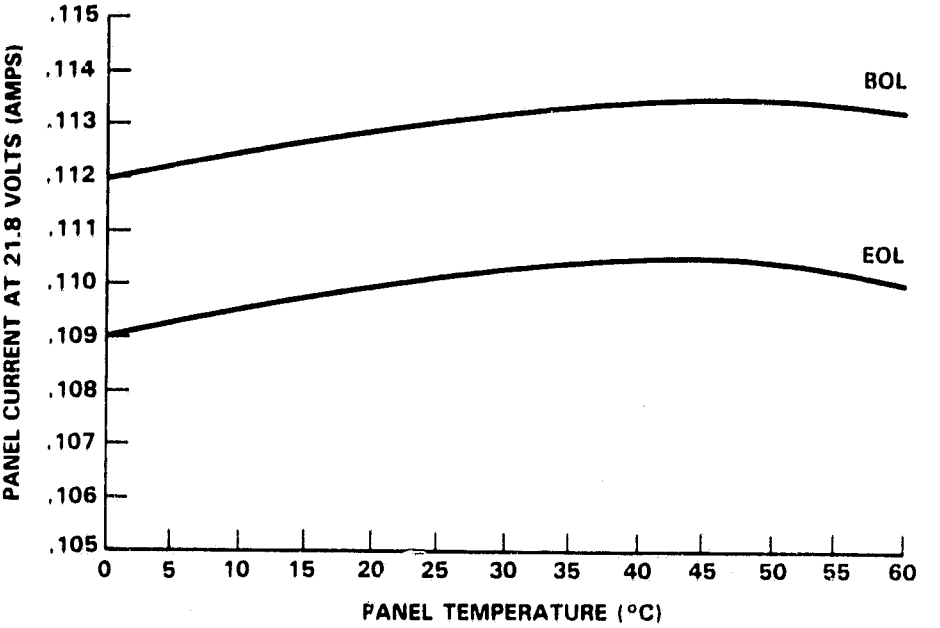

FIGURE 16. GaAs PANEL OUTPUT VS TEMPERATURE
AT AMO SOLAR ILLUMINATION

SEASONAL AND ACCUMULATIVE DEGRADATION EFFECTS

The output current of the solar cell panels in flight will vary from the AMO output because the solar intensity incident upon San Marco D/L, as well as other earth orbiting spacecrafts, will vary seasonally with the sun-earth distance. The intensity will change from 130.9mW/cm² at summer solstice to 139.9mW/cm² at winter solstice which causes the solar array output at summer solstice to be approximately 3.4% below the array output at AMO illumination[14].

Ultraviolet radiation from the sun will reduce the transmissivity of solar cell coverglasses and coverglass adhesive, therefore, degrading the solar array output. However, this degradation is minor because solar cell coverglasses have thin film optical coatings that reflect ultraviolet radiation. The type of UV filter for the San Marco D/L solar cells (Si and GaAs) has a cut-on (50% rejection) wavelength of .35 micrometers. According to qualification tests[7] performed on this cell/cover assembly type, the power loss due to the residual UV transmission after 2330 sun hours will be 1.8%. The net array current loss due to UV irradiation over the life of San Marco D/L should converge to approximately 2.0%.

Thermal vacuum cycling of a solar array panel results in a degradation of electrical performance because of an increase in the electrical resistance of solar cells and cell interconnects with material fatigue. This degradation depends on the number of cycles and the temperature extremes[14]. The San Marco D/L solar cell panels are exposed to a relatively benign thermal environment; thus, the degradation factor associated with temperature cycling is not expected to exceed 1%.

WINDOW TRANSMISSION AND SHADOWING EFFECTS

The windows, which allow the sun to illuminate the solar array panels, are covered with mica sheets (.05 to .08 mm thick). A cover is required because of the aerodynamic design limitations previously discussed. The ruby mica sheets are more desirable than other materials because of trade-off considerations between the mechanical, thermal and optical properties of the materials[4]. Nevertheless, the presence of the mica covers results in transmission losses that reduces the available

solar array current. The transmissivity of the ruby mica sheets is a function of the wavelength of incident light (Figure 17). When this transmissivity curve is averaged over a typical solar cell's response to the AMO solar spectrum, the resulting transmissivity is 0.86. It has been previously shown[4] that the transmissivity of the ruby mica sheets can be considered independent of the charged-particle and UV radiation environments for a low equatorial orbit and a lifetime of 1 year. However, the transmissivity of the mica sheets will decrease with increasing sun angle, as shown in Figure 18. In order to simplify analysis that will be performed in the next section, the mica transmissivity should be expressed in terms of direction cosine. Polynomial regression analysis (a least squares method) has been used to define a functional relationship between the mica transmissivity and the cosine of the angle of incidence.

Because of the gap between the outer shell of the spacecraft and the solar array panels, the window frames will shadow the solar cell panel. The spacecraft outer shell (at the top, bottom and sides of the window) can shadow the panel; thus, there is a maximum view angle of the sun with respect to the equator and the meridian plane. The maximum view angles, beyond which a panel loses all power due to window frame shadows are:

$$\psi_{max} = \pm 50^\circ \text{ and } \beta_{smax} = \pm 29^\circ$$

where, ψ and β are defined in Figure 19. β_{SMAX} has been determined taking into account the contribution of 3 parameters: (1) the maximum sun-declination with respect to the earth's equatorial plane, (2) the inclination of the spacecraft's orbital plane, and (3) the tolerance on the spin axis direction.

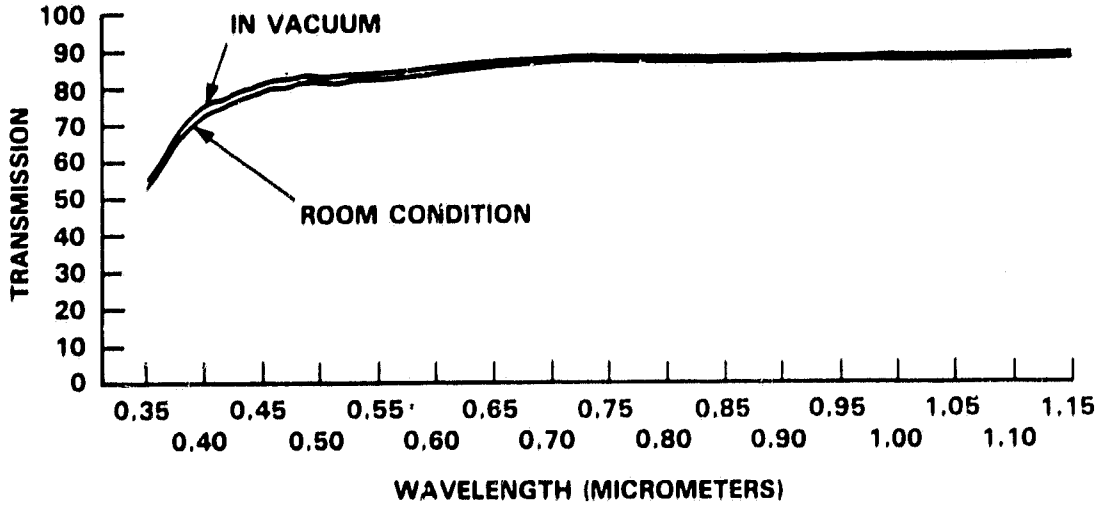

FIGURE 17. RUBY MICA TRANSMISSIVITY VS LIGHT WAVELENGTH

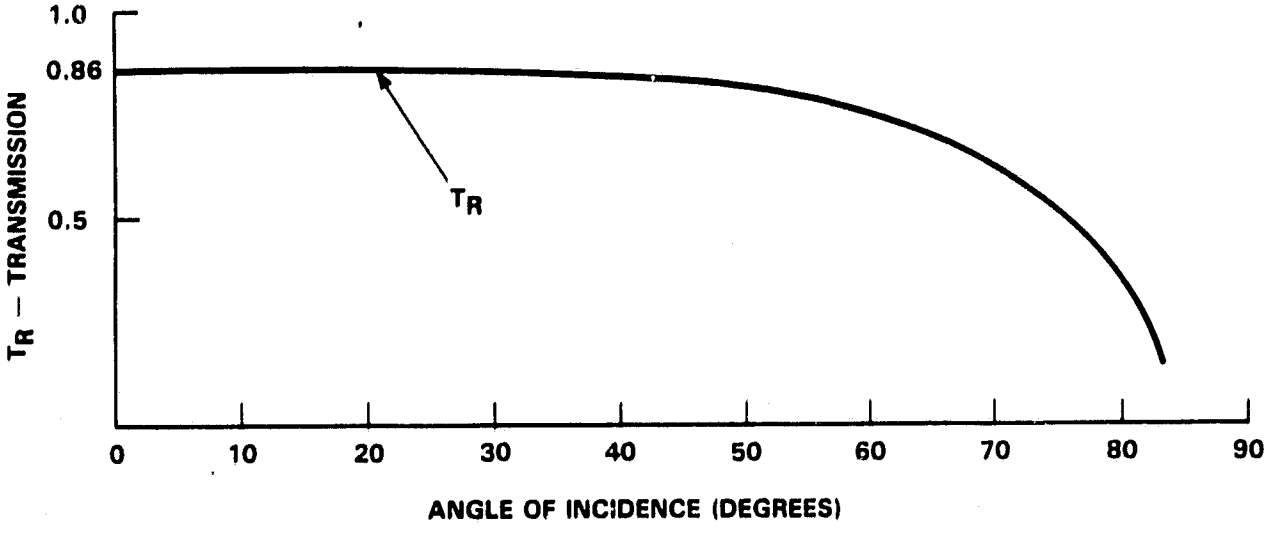

FIGURE 18. RUBY MICA TRANSMISSION VS SUN ANGLE

$\vec{n}$ = THE PANEL'S NORMAL UNIT VECTOR
β_s = ANGLE BETWEEN THE SUN LINE AND THE SPACECRAFT'S EQUATORIAL PLANE
β_o = ANGLE BETWEEN THE PANEL'S NORMAL AND THE SPACECRAFT'S EQUATORIAL PLANE
Φ_o = ANGLE BETWEEN THE SPACECRAFT'S × AXIS AND THE PROJECTION OF THE PANEL'S NORMAL IN THE SPACECRAFT'S EQUATORIAL PLANE
Φ = SPIN ANGLE
Ψ = $\Phi_o + \Phi$

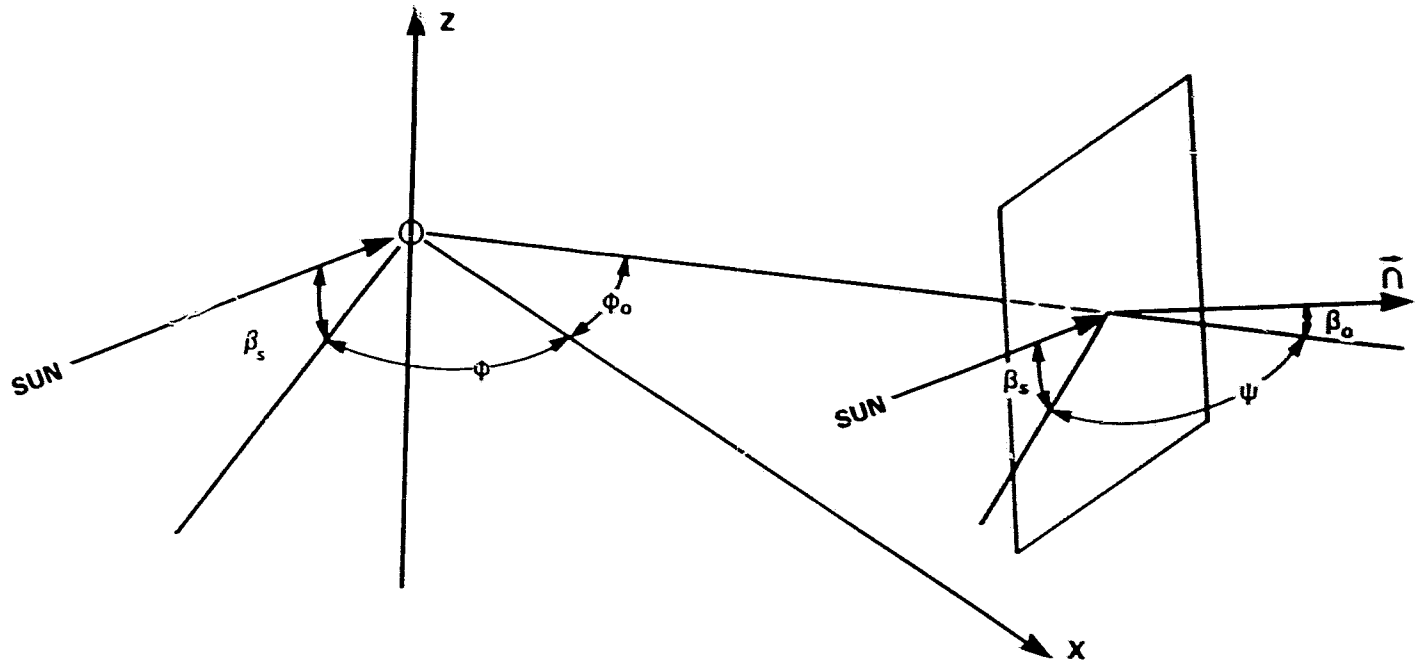

FIGURE 19. DEFINITION OF VIEW ANGLES

SPIN-AVERAGED ARRAY PERFORMANCE

The normal incidence AMO performance of the Si and GaAs panels, the various solar array power loss factors, and the sun angle dependent parameters have been previously defined. The actual inflight solar array power profile can now be computed. The net solar array output is the sum of the outputs of the individual panels for the given spacecraft orientation with respect to the sun.

$$P_{Array}(\beta_s, \phi) = \sum_{i=1}^{28} P_i(\beta_s, \phi)$$

where β_s is the angle between the sunline and the spacecraft's equatorial plane and Φ is the spacecraft's spin angle. The output of an individual panel is the product of: (1) the output of the panel when the sun is at normal incidence (including all sun angle independent power loss factors); (2) the direction cosine between the sun line and the panel's normal; and (3) the mica window transmission as a function of the direction cosine between the sunline and the panel's normal.

$$P_i(\beta_s, \phi) = P_o \bullet [\text{Direction Cosine}] \bullet [T_R \text{ (Direction Cosine)}]$$

Since T_R (as a function of direction cosine) and P_O are known, the problem is reduced to calculating the direction cosine between the sun line and the normal to each individual panel.

The direction cosine between the sun and the spacecraft solar array panels can be easily calculated using rotation matrices[15]. As applied to the San Marco D/L solar array, the unit vector in the direction of the panel's normal interms of a unit vector in the direction of the sun (+X direction) is:

$$\begin{pmatrix} X_o \\ Y_o \\ Z_o \end{pmatrix} = \begin{pmatrix} \cos\phi_o & -\sin\phi_o & 0 \\ \sin\phi_o & \cos\phi_o & 0 \\ 0 & 0 & 1 \end{pmatrix} \begin{pmatrix} \cos\beta_o & 0 & \sin\beta_o \\ 0 & 1 & 0 \\ \sin\beta_o & 0 & \cos\beta_o \end{pmatrix} \begin{pmatrix} 1 \\ 0 \\ 0 \end{pmatrix}$$

Φ_O is the angle between the spacecraft's x axis and the projection of the panel's normal in the spacecraft's equatorial plane, as defined for each panel in Figure 2. β_O is the angle between the spacecraft's equatorial plane and the panel's normal (+9° and −9° for panels in the lower and upper loops, respectively). The unit vector in the direction of the panel's normal for an arbitrary spacecraft orientation with respect to the sun is:

$$\begin{pmatrix} X(\beta_s, \phi) \\ Y(\beta_s, \phi) \\ Z(\beta_s, \phi) \end{pmatrix} = \begin{pmatrix} \cos(\phi + \phi_0) & -\sin(\phi + \phi_0) & 0 \\ \sin(\phi + \phi_0) & \cos(\phi + \phi_0) & 0 \\ 0 & 0 & 1 \end{pmatrix} \begin{pmatrix} \cos(\beta_s + \beta_0) & 0 & \sin(\beta_s + \beta_0) \\ 0 & 1 & 0 \\ -\sin(\beta_s + \beta_0) & 0 & \cos(\beta_s + \beta_0) \end{pmatrix} \begin{pmatrix} 1 \\ 0 \\ 0 \end{pmatrix}$$

Φ is the spacecraft's spin angle. β_S is the angle between the sun line and the spacecraft's equatorial plane. The direction cosine is the dot product of the unit vector along the sun line with the unit vector in the direction of the panel's normal.

$$\text{Direction Cosine} = (1 \quad 0 \quad 0) \bullet \begin{pmatrix} X(\beta_s, \phi) \\ Y(\beta_s, \phi) \\ Z(\beta_s, \phi) \end{pmatrix}$$

$$= X(\beta_s, \phi) = \cos(\beta_s + \beta_0) \cos(\phi + \phi_0)$$

Several conditions are imposed on the above calculation of the direction cosine. As discussed in the previous section, if $\cos(\Phi + \Phi_O) < \text{Cos}(50°)$ then the direction cosine is set equal to zero. Also, if the calculation results in a negative direction cosine (such as when the rear of the panel is facing the sun) the direction cosine is set equal to zero. With the above constraints, the net solar array output for a given spacecraft orientation is calculated from the following expression.

$$P_{\text{Array}}(\beta_s, \phi) = P_o^{Si} \sum_{i = 1 \text{ to } 28} X_i(\beta_s, \phi)\, T_R\,(X_i(\beta_s, \phi))$$

$$- P_o^{Si} \sum_{i = 3 \text{ and } 24} X_i(\beta_s, \phi) T_R\,(X_i(\beta_s, \phi))$$

$$+ P_o^{GaAs} \sum_{i = 3 \text{ and } 24} X_i(\beta_s, \phi)\, T_R\,(X_i(\beta_s, \phi))$$

Where the above is written in a form which is convenient for evaluating the contribution of the 2 GaAs panels to the total array output. Two computations have been performed and shown in Figure 20: (a) assuming all the panels are Si (the first term only) and (b) the real case, 2 Si panels are replaced by GaAs panels.

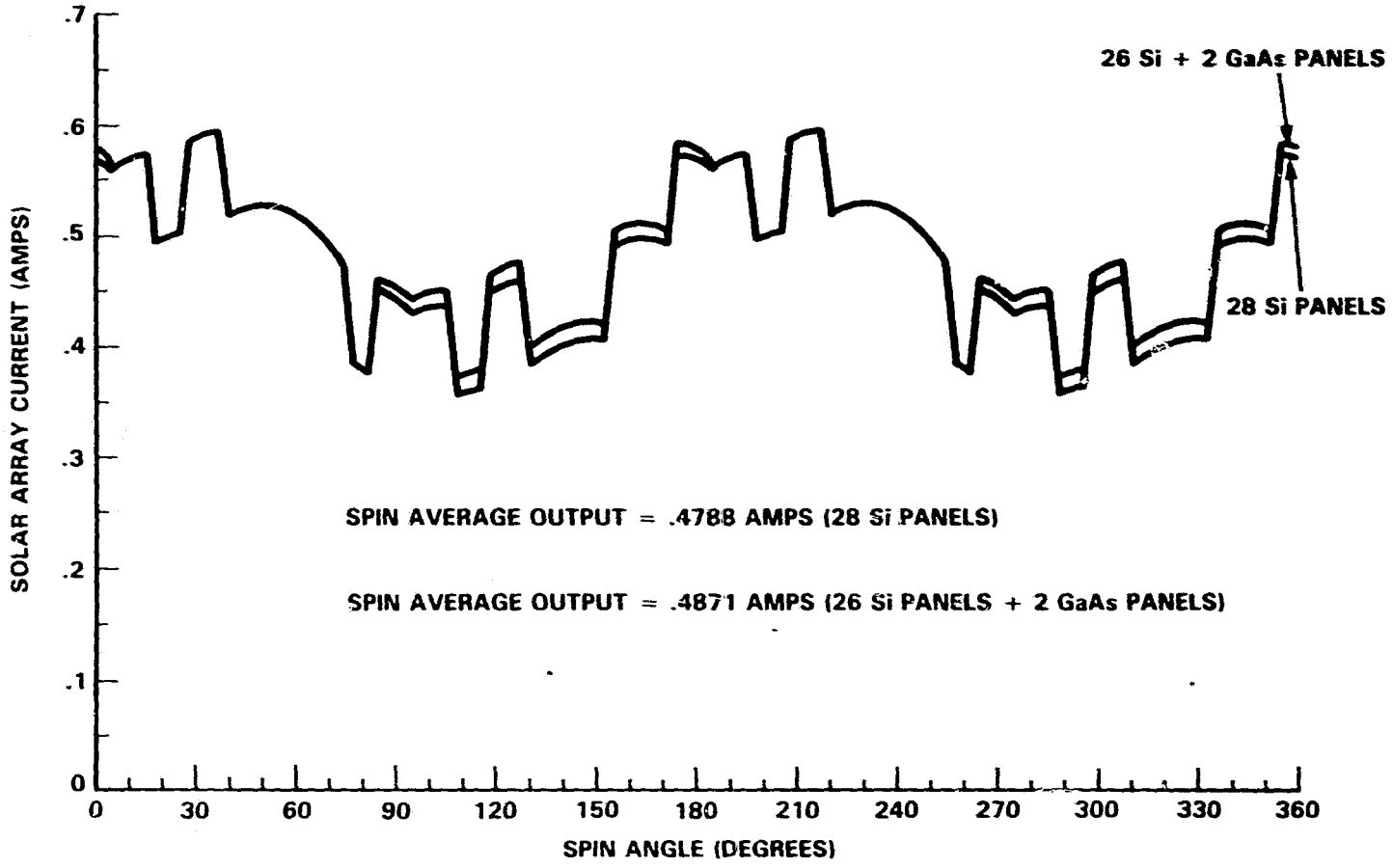

FIGURE 20. SOLAR ARRAY PERFORMANCE AT 21.8V, 28°C, AND SUMMER SOLSTICE ILLUMINATION

SHADOWING BY MOMENT OF INERTIA BOOMS

As shown in Figure 21, 4 booms are mounted along the equator of San Marco D/L for inertial balance. At certain sun angles the booms will shadow the solar array panels, therefore, reducing the spin-averaged array output. The losses in available power due to shadowing of the solar array by the moment of inertia (MOI) booms have been quantified by using computer graphic techniques to model all possible orientations of the spacecraft as viewed by the sun[15]. The identical procedure used in the previous section to orientate unit vectors is used here to orientate all the coordinate points, lines, and surfaces that are required to sketch the solar array panels and MOI booms. Once the points have been rotated to the given sun angle (β_S) and spin angle (ϕ), the solar array panels and booms are drawn by a programmable x-y plotter.

Shadows across the solar array panels may be observed for any given β_S and ϕ. The panel output at that orientation is reduced by a factor equal to the fraction of cell area shadowed on the worst case shadowed series cell. As an example, if half the area on all 56 series Si cells of a panel were shadowed, the output of the panel is reduced by 1 half. however, if 1 Si cell is completely shadowed and the remaining 55 series Si cells are not shadowed, the output of a panel is reduced to zero. The output of a panel is reduced over its shadowed range of ϕ by truncating the direction cosine calculated in the previous section.

When the sun line is in the spacecraft equatorial (x-y) plane and normal to the equator of the spacecraft, no solar array panel is shadowed by the booms. As shown in Figure 22, the shadow is always between the upper and lower loops of solar array panels. Therefore, the solar array output is not reduced from that shown in Figure 20. For a sun angle of $\beta_S = \pm 10°$, shadowing of certain solar array panels will occur as the spacecraft spins (Figure 23). The resulting decrease in the spin-averaged solar array output due to shadowing by the booms is approximately 7 percent (Figure 24). The bottom and top profiles are the respective solar array outputs with and without the booms.

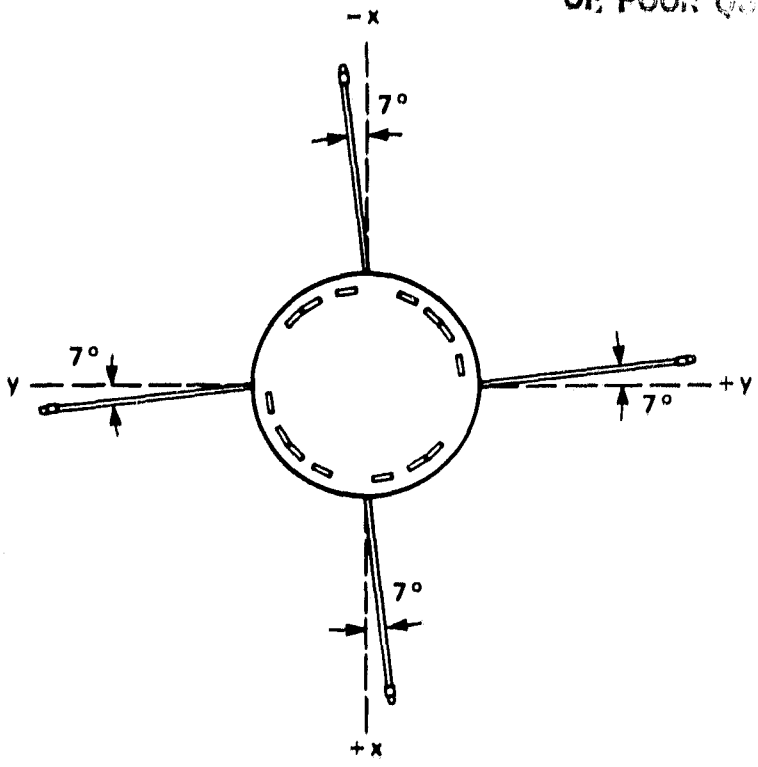

FIGURE 21. CONFIGURATION OF MOI BOOMS

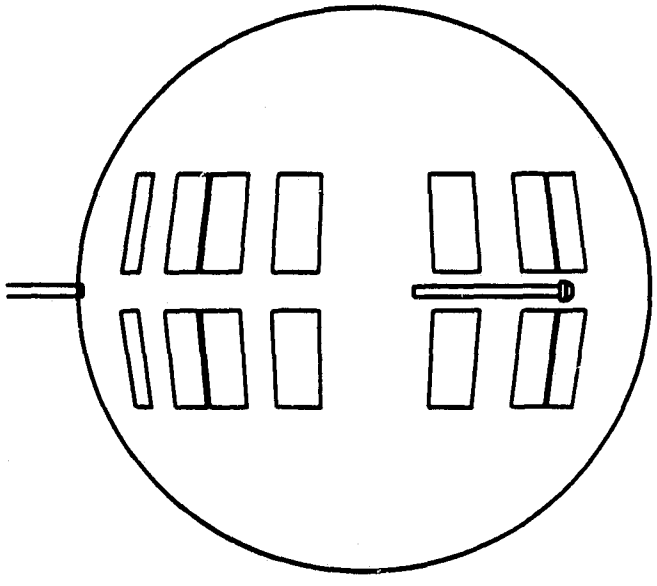

FIGURE 22. SAN MARCO D/L SOLAR ARRAY SHADOWING STUDY
SUN ANGLE = 0 DEGREES
SPIN ANGLE = 10 DEGREES

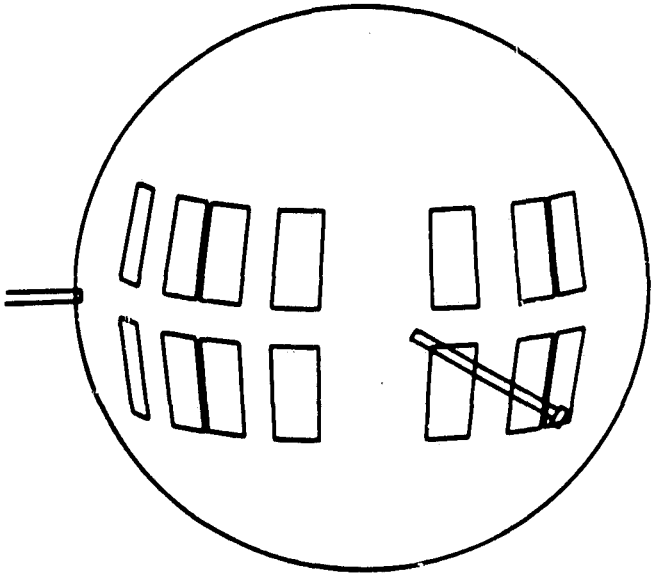

FIGURE 23. SAN MARCO D/L SOLAR ARRAY SHADOWING STUDY
SUN ANGLE = 10 DEGREES
SPIN ANGLE = 10 DEGREES

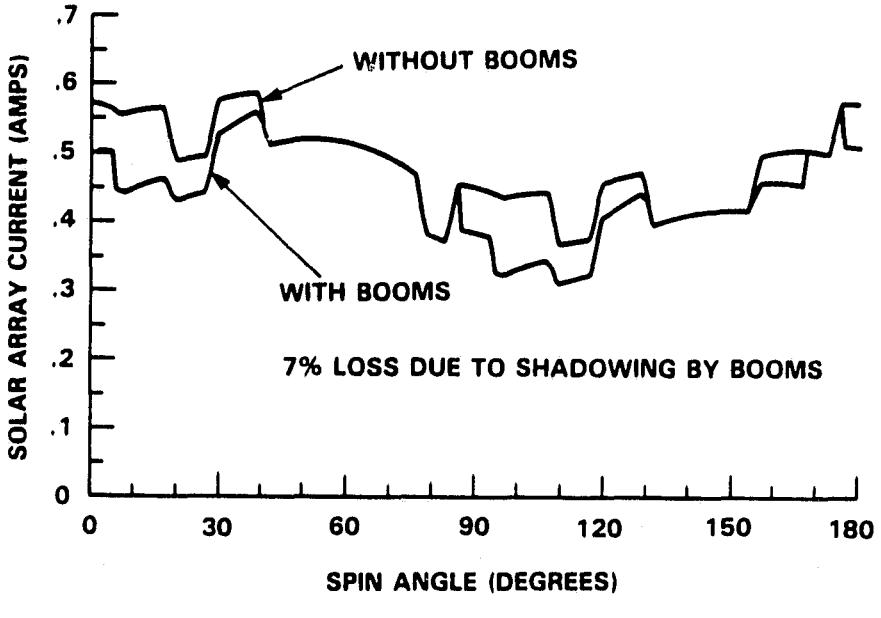

FIGURE 24. SOLAR ARRAY PERFORMANCE WITH AND WITHOUT MOI BOOMS
SUN ANGLE = 10°

The shadowing analysis was performed for various sun angles. It was found that the solar array power losses due to shadowing by the booms will increase from 0% for $\beta_S = 0°$ to a worst case of 7% for $\beta_S \pm 10°$. Then the losses will decrease for larger sun angles. At the sun angle limit $\beta_S = \pm 29°$), the shadowing losses will be approximately 4 percent.

SUMMARY

The San Marco D/L solar array system is non-conventional and quite unique due to constraints imposed on the dimensions and location of the solar cell panels. In order to satisfy the drag balance requirements, the solar array panels are placed inside the spacecraft behind mica windows. The performance of this solar array system has been evaluated. The San Marco D/L solar array system will provide less than 12 watts available spin-averaged power at the best case sun angle; and at least 30% more illumination losses are experienced than with conventional spacecraft solar array system designs. The spacecraft power demand is such that the on-board experiments must be duty cycled in order to balance the power budget.

The San Marco D/L will be one of the first spacecraft to use GaAs solar cell panels as essential elements in the solar array system. Therefore, the flight experiment comparing the in-flight performance of 1 GaAs panel and 1 Si panel represents a valuable source of information for the space photovoltaic community. The preflight performance of the 2 panels have been compared; at 28 °C and AMO solar illumination, the peak power output of the Si panel is approximately 20% less than the peak power output of the GaAs panel. The spacecraft telemetry system will provide the operating temperature, operating voltage and output current of both panels during flight.

REFERENCES

1. R. Adkins (project manager), "Execution Phase Project Plan for the San Marco-D International Cooperative Project" NASA GSFC, June 1979.
2. M. Di Ruscio, "The SMD/L Power Supply System Design Data", University of Rome, CRA Technical Paper 143, October 1980.
3. L. Broglio, "Aspetti Scientifici e Tecnici del Satellite San Marco", Atti del Centro Ricerche Aerospaziali, University of Rome, n. 15b, 1967.
4. C. Arduini and G. Ravelli, "A Non-Conventional Solar Array for the San Marco C Satellite", International Colloquium on Solar Cells, Toulouse, July 1970.
5. J.H. Day, "Preflight Study of the San Marco D/L GaAs Solar Cell Panels", NASA LeRC 6th Space Photovoltaics Research and Technology (SPRAT) Meeting, October 1983.
6. R.C. Knechtl:, G.S. Kamath, J. Ewan and R.Y. Loo, "Development of Space-Qualified GaAs Solar Cells", Hughes Research Laboratories, Research Report No. 534, April 1980.
7. L.J. Goldhammer, "Qualification and Characterization of the K7 Solar Cell" Final Report, Hughes Research Laboratories, May 1978.
8. Spectrolab, "Preliminary Data Package: San Marco D/L Solar Arrays", July 1980.
9. E.G. Stassinopoulos, "Analysis of the San Marco D/L Orbit Radiation Exposure", NASA GSFC X-601-79-0, December 1978.
10. H.Y. Tada, J.R. Carter, Jr., B.E. Anspaugh, and R.G. Downing, "Solar Cell Radiation Handbook", 3rd Edition, NASA JPL Publication 82-69, November 1982.
11. J.W. Wilson, J.J. Smith, and G.H. Walker, "On the Validity of Equivalent Electron Fluence for the GaAs Solar Cells", IEEE Photovoltaic Specialists Conference, September 1982.
12. B.E. Anspaugh, R.G. Downing, T.F. Miyahira, and R.S. Weiss, "Electrical Characteristics of Spectrolab BSF, BSR, Textured 290-Micron Solar Cells (K7) as a Function of Intensity, Temperature and Irradiation", NASA JPL Publication 78-15, Volume VIII, September 1979.

13. B.E. Anspaugh, R.G. Downing, T.F. Miyahina, and R.S. Weiss, "Electrical Characteristics of Hughes Liquid Phase Epitaxy Gallium Arsenide Solar Cells as a Function of Intensity, Temperature and Irradiation", NASA JPL Publication 78-15, Volume XIV, November 1981.

14. H.S. Rauschenbach, "Solar Cell Array Design Handbook", Van Nostrand Reinhold Co., 1980.

15. E.M. Gaddy, "Computing the Projected Area of a Spacecraft Solar Array with Matrices", 18th Intersociety Energy Conversion Engineering Conference, August 1983.